Geophysical Research Letters

RESEARCH LETTER
10.1029/2018GL079330

Key Points:
- First observation on transport of solar wind protons scattered from lunar magnetic anomaly into the near wake region
- Forward scattering by magnetic anomaly at South Pole-Aitken basin for high solar zenith angle
- The flux is estimated to be $\sim 5 \times 10^{-4}$ of the solar wind proton flux

Supporting Information:
- Supporting Information S1

Correspondence to:
M. B. Dhanya and A. Bhardwaj,
mb_dhanya@vssc.gov.in;
abhardwaj@prl.res.in

Citation:
Dhanya, M. B., Bhardwaj, A., Alok, A., Futaana, Y., Barabash, S., Wieser, M., et al. (2018). First observation of transport of solar wind protons scattered from magnetic anomalies into the near lunar wake: Observations by SARA/Chandrayaan-1. *Geophysical Research Letters*, *45*, 8826–8833. https://doi.org/10.1029/2018GL079330

Received 22 JUN 2018
Accepted 23 AUG 2018
Accepted article online 29 AUG 2018
Published online 14 SEP 2018

©2018. American Geophysical Union. All Rights Reserved.

First Observation of Transport of Solar Wind Protons Scattered From Magnetic Anomalies Into the Near Lunar Wake: Observations by SARA/Chandrayaan-1

M. B. Dhanya[1], Anil Bhardwaj[2], Abhinaw Alok[1], Yoshifumi Futaana[3], Stas Barabash[3], Martin Wieser[3], Mats Holmström[3], and Peter Wurz[4]

[1]Space Physics Laboratory, Vikram Sarabhai Space Centre, Trivandrum, India, [2]Physical Research Laboratory, Ahmedabad, India, [3]Swedish Institute of Space Physics, Kiruna, Sweden, [4]Physikalisches Institut, University of Bern, Bern, Switzerland

Abstract We report the first observational evidence for the transport of the solar wind protons scattered from the lunar magnetic anomaly (LMA) into the near wake region from SWIM/Sub-keV Atom Reflecting Analyzer (SARA) aboard Chandrayaan-1. These protons with high angular spread are observed in the near wake region for specific orientations of interplanetary magnetic field. The typical energy range is 600–1,000 eV, which is either smaller or comparable to that of solar wind. Using our backtracing model, the source region of these protons is found to be the large LMA at South Pole-Aitken basin on the dayside, suggesting that these are solar wind protons forward scattered from LMA at the South Pole-Aitken. The flux of these protons is $\sim 5 \times 10^{-4}$ of the solar wind proton flux, which is comparable to the proton population in near wake due to other known processes. Such protons can significantly affect the electromagnetic environment in near wake region.

Plain Language Summary The understanding of solar wind interaction with the Moon and the ensuing plasma dynamics are still evolving. The near lunar wake refilling by solar wind protons are a recent discovery, and a few processes are now known to play a role. The small-scale crustal magnetic fields on the Moon can also cause scattering of the impinging solar wind protons back to space. This paper shows for the first time that solar wind protons scattered from lunar magnetic regions on dayside can get transported to the nightside of the Moon, thereby contributing an additional process of plasma refilling in the near wake region. The results have direct applications to near lunar plasma environment and to any atmosphere-less body with no global magnetic field, such as asteroids and several planetary satellites. The findings have impact on space plasma physics, as well as lunar and planetary science communities.

1. Introduction

The Moon is an airless nonmagnetized planetary object. However, there are regions of crustal magnetic fields with strengths up to few hundred nano-Tesla, which are known as lunar magnetic anomalies (LMA; Mitchell et al., 2008, and references therein). The magnetic anomalies have been found to deflect a significant fraction of the solar wind (up to 50%) impinging on the Moon (Bhardwaj et al., 2015; Lue et al., 2011; Poppe et al., 2017; Saito et al., 2010).

The interaction of solar wind plasma with the Moon leaves a cavity at the downwind side of the Moon known as lunar plasma wake. Recent observations have shown that there are several processes, kinetic in nature, which transport solar wind plasma to the near wake region (100–200 km from the surface). The processes include direct transport of solar wind to wake by finite gyroradius (Dhanya et al., 2013; Nishino, Maezawa, et al., 2009) and diffusion parallel to the interplanetary magnetic field (IMF; Futaana et al., 2010). The indirect transport include the entry of solar wind scattered from dayside lunar surface to the near wake region (Nishino, Fujimoto, et al., 2009; Wang et al., 2010) and also the solar wind scattered from Earth's bow shock (Nishino et al., 2017). Further, new population of protons is found in the near lunar wake whose source(s) is(are) yet to be identified (Dhanya et al., 2016, 2017; Vorburger et al., 2016).

It is plausible that the solar wind protons scattered from LMA enter the near wake region and hence a significant source for near wake refilling (Dhanya et al., 2016; Poppe et al., 2017). However, there is no direct

source: https://doi.org/10.7892/boris.122698 | downloaded: 12.10.2024

observational evidence so far for such a process, and also, the energy and flux of such a population in near wake are not known. In the following, we demonstrate the first observational evidence for this process.

2. Instrument and Data

The Sub-keV Atom Reflecting Analyzer (SARA) experiment on Chandrayaan-1 consisted of an ion-mass analyzer, namely, Solar Wind Monitor (SWIM), that operated in the energy range of 100–3,000 eV/q ($\triangle E/E \sim 7\%$; Barabash et al., 2009; Bhardwaj et al., 2005). SWIM had a fan-shaped field of view with 16 angular pixels of resolution ~3.5° (elevation) × 10° (azimuth), depending on the viewing direction. Assisted by the nadir-pointing spacecraft motion, the field of view covers ~ 2π within half of the orbit. More details about SWIM are given in previous publications (Bhardwaj et al., 2012; Dhanya et al., 2013, 2016; Futaana et al., 2010). Chandrayaan-1 was in a circular polar orbit around the Moon and operated at altitudes of ~100 and ~200 km. Observations made by SWIM when Moon was located outside the Earth's bow shock have been used for the analysis reported here.

For the upstream solar wind plasma parameters, such as solar wind velocity and IMF, level-2 data of the solar wind electron, proton, and alpha monitor (SWEPAM), and magnetometer (MAG) instruments onboard the Advanced Composition Explorer (ACE) satellite are used. Since ACE makes measurements at the L1 point of Sun-Earth system, we time shifted the solar wind parameters to the location of the Moon (Dhanya et al., 2016). The convective electric field (CEF) of the solar wind is derived from the solar wind velocity (V_{sw}) and IMF (B_{IMF}) as $\vec{E_c} = -\vec{V_{sw}} \times \vec{B_{IMF}}$.

For the analysis, we have used an aberrated lunar-centered solar ecliptic (aLSE) coordinate system. The aLSE coordinate system has the x axis antiparallel to the solar wind velocity (V_{sw}), the z axis is toward the ecliptic north, and the y axis completes the right-handed coordinate system (illustrated in Figure 1 of Dhanya et al., 2016).

A backtracing model that is developed for calculating the trajectories of the protons observed by SWIM back in time, where the Lorentz force equation is solved by the Euler method (details in Dhanya et al., 2016), is used here. The electric field includes CEF and an inward electric field of ~0.7 mV/m in the wake boundary region with a width of $0.25 \times R_L$, where R_L is the lunar radius (Halekas et al., 2005; Nishino et al., 2009). The magnetic field is essentially the IMF, which is enhanced by a factor of 1.5 inside the wake (Colburn et al., 1967). The backtracing calculation proceeds until either the particles hit the surface of the Moon ($r < 1738$ km; where r is the position vector of the particles in aLSE coordinates) or travel sufficiently larger distance upstream of the Moon ($r > 5{,}000$ km).

3. Observation

Figures 1a–1c show the orbit geometry for the Moon on 20 April 2009 and for the Chandrayaan-1 orbit 1977 during 09:30 UT to 11:28 UT on 20 April 2009. As seen from Figure 1a, the Moon was in the undisturbed solar wind flow upstream of the Earth's bow shock. During the orbit 1977, Chandrayaan-1 entered the nightside of the Moon crossing the South Pole and moved to the dayside crossing the North Pole (Figure 1b). Close to the terminator and more into the nightside, Chandrayaan-1 was moving close to the biggest LMA region cluster located in the Southern Hemisphere at the north side of the South Pole-Aitken basin (SPA). The magnetic anomaly located at SPA (termed as SPA LMA, hereafter) is located on the far side of the Moon and has a spatial extension in longitude from ~150° to ~210°. During this observation, the SPA LMA was on the sunlit side of the Moon. The subsolar point during our observation was at ~250° longitude (Figure 1c). The solar zenith angle (SZA) at the LMA cluster during our observation was in the range of ~ 40°–90° due to the spatial extent of the LMA cluster over the lunar surface.

The energy-time spectra observed by SWIM juxtaposed with the real-time solar wind parameters during the orbit 1977 of Chandrayaan-1 are shown in Figures 1d–1j. The signal observed by SWIM between 10:42 UT and 11:15 UT, marked as A in Figure 1d, corresponds to solar wind observed on the dayside of the Moon. The dayside equator crossing by Chandrayaan-1 was at ~11:00 UT. The population B are the protons observed in the near and deep lunar wake (~09:48 to 10:10 UT). These protons have an energy of ~1,300 eV that is comparable to that of the dayside solar wind (A) and are confined in almost three directions bins (bins 5–7) of SWIM (Figure 1e). Such protons have been studied before and are known to enter the near wake region by a number of processes (Dhanya et al., 2013, 2016; Futaana et al., 2010; Nishino et al., 2009, 2009).

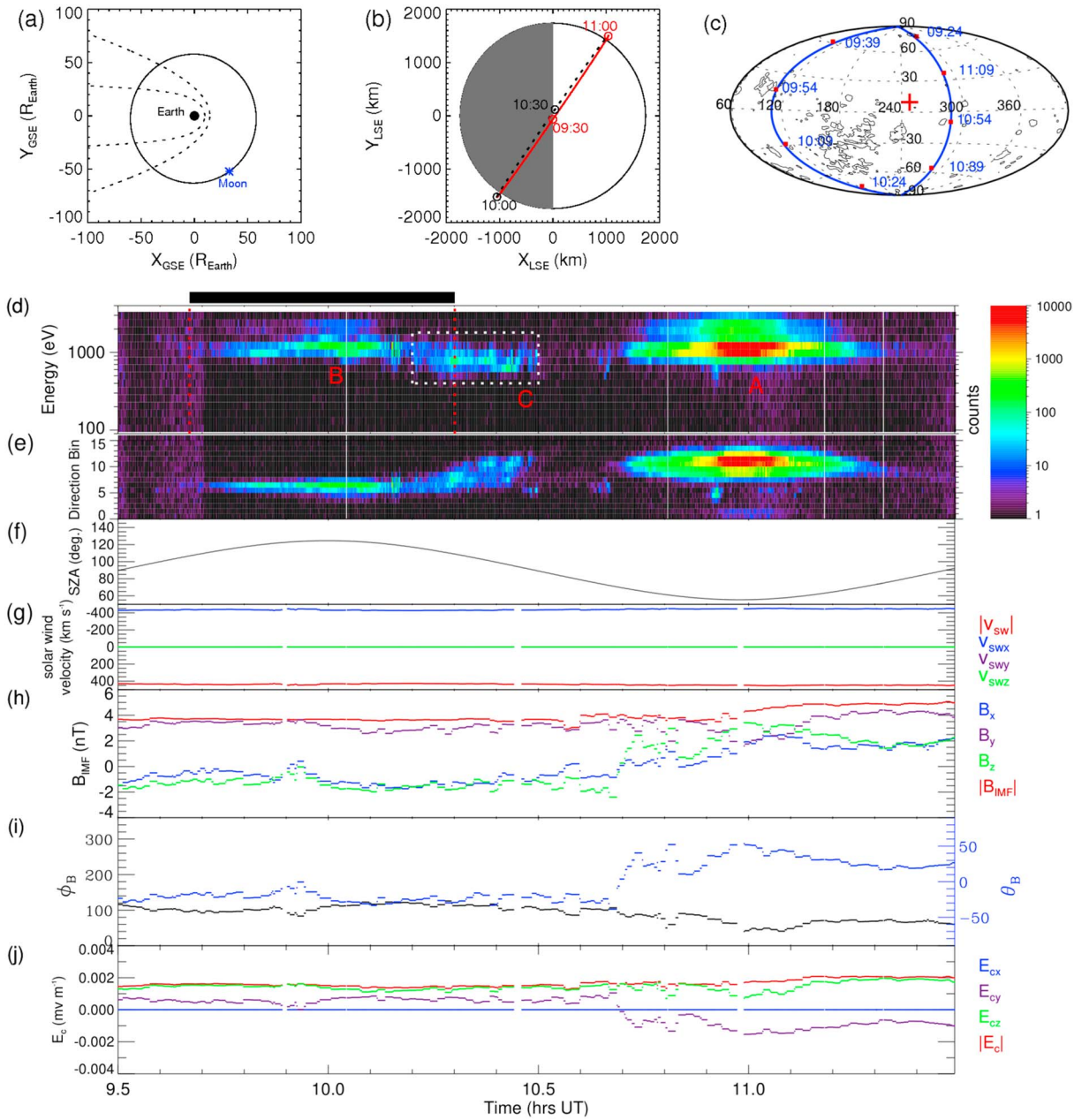

Figure 1. (a) Orbit of the Moon around the Earth for April 2009 projected on the *x-y* plane of the Geocentric Solar Ecliptic (GSE) coordinates. GSE has its origin on the Earth center, the *x* axis is toward the Sun, *z* axis toward the ecliptic north, and the *y* axis completes the right-handed coordinate system. Estimated boundaries of Earth's magnetosphere and bow shock are shown. Position of the Moon on 20 April 2009 is indicated by the asterisk symbol (blue color). (b) Orbit of Chandrayaan-1 around the Moon during the orbit 1977 on 20 April 2009 (~09:30 UT to 11:30 UT), projected on the *x-y* plane of lunar-centered solar ecliptic (LSE) coordinates as viewed from $+z_{LSE}$. The red solid curve indicates the part of orbit with $z_{LSE} > 0$, and black dotted curve is with $z_{LSE} < 0$. The position of Chandrayaan-1 at four time instants are also indicated. (c) Chandrayaan-1 orbit 1977 in the hammer projection of lunar map. The black contours represent the magnetic field magnitude (2 nT at an altitude of 30 km) of the anomalies based on Purucker and Nicholas (2010). The projection is roughly centered at the subsolar point, which is indicated by the symbol "+" in red color. (d) Energy-time spectrogram from SWIM observations for the orbit 1977 of Chandrayaan-1. The horizontal axis shows time in hours universal time. The black-filled box on the top indicates the time interval when Solar Wind Monitor (SWIM) made observations in lunar wake (~09:42 to ~10:18 UT). A pair of dotted vertical lines in red color mark the wake entry and exit timings for Chandrayaan-1. Different population of ions observed by SWIM in this orbit are indicated as *A*, *B*, and *C*. The white colored rectangle is used to highlight the population C observed during the day-night terminator crossing and extending into the wake. (e) Direction-time spectrogram from the SWIM observations for the same orbit. The vertical axis shows the 16 direction bins in which ions are observed by SWIM. Direction bin 0 refers to close to nadir, and direction bin 15 refers to close to zenith. (f) Solar zenith angle. (g) Solar wind velocity: magnitude (V_{sw}) and the components (V_x, V_y, and V_z). (h) Interplanetary magnetic field magnitude ($|B_{IMF}|$) as well as the components B_x, B_y, and B_z. (i) The azimuth (ϕ_B) and elevation (θ_B) angles of B_{IMF}. (j) Convective electric field (E_c) of the solar wind: the magnitude $|E_c|$ and the components E_x, E_y, and E_z. The solar wind parameters shown in the panels (g)–(j) are in aberrated LSE coordinates.

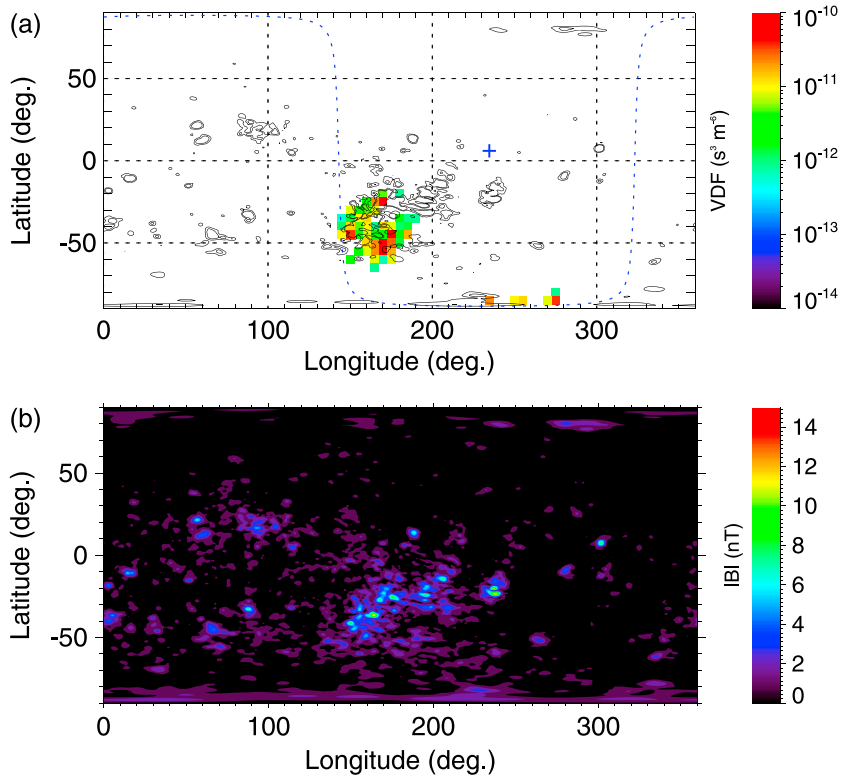

Figure 2. (a) Map in selenographic coordinates showing the location of origin of the protons of population *C* at the end of backtracing. The map is genenerated using the 3-D backtracing model. The point of intersection of the particle trajectories with the lunar surface is binned to grid cells of size 5° × 5° in the selenographic coordinates. The color bar represents the phase space density of the protons. The subsolar point during the observation of population *C* is indicated by the symbol "+" (blue color). The blue-colored dotted curves indicate the day-night terminator. The lunar crustal magnetic fields are shown as black contours for magnitudes of 2 and 3 nT (Purucker & Nicholas, 2010). (b) The global map of lunar magnetic anomaly at an altitude of 30 km based on Purucker and Nicholas (2010).

The population *C* that is observed close to the day-night terminator extending into the near wake region (∼10:10 to 10:30 UT) has been recorded in several viewing directions of SWIM (Figure 1e). This population is quite different from population B in terms of the angular spread (bins 5–13) of these ions. Since higher direction bins corresponds to directions more toward zenith, this is indicative that the ions belonging to the population *C* could be transported from some distant location. Also, the energy of these ions are ∼800 eV that is lower than both the populations *A* and *B*. The ions of population *C* is of interest and is analyzed further.

During the observation of the population *C*, the SZA was in the range of ∼80°–120° (Figure 1f), solar wind had fairly constant speed of ∼450 km/s (Figure 1g), and IMF had almost a constant field strength of ∼4 nT with a dominant *y* component (B_y; Figure 1h). It is seen from Figure 1i that during the observation of population *C*, the elevation angle of IMF, $\theta_B \sim -20°$ and azimuth angle, $\phi_B \sim 120°$. The solar wind CEF ($|E_c|$) was ∼0.001 mV/m with a dominant positive *z* component (Figure 1j). SWIM had time-of-flight section with a mass resolution $m/\Delta m \sim 1.5$. Mass analysis of ion population *C* confirms that these ions are basically protons with $m/q = 1$.

To get an insight into the source of these protons belonging to the population *C* observed over a range of direction bins and specific energy bins of SWIM, the trajectories of the protons are traced back in time using the backtracking model. Backtracing shows that a significant population of the protons are originated from the lunar dayside surface. The velocity distribution function of the protons after backtracing is presented in Figure 2a, where the location of the particles that hit the lunar surface at the end of backtracing is binned into the grid cells of size 5° × 5° in selenographic coordinates. In comparison, the global map of the lunar crustal magnetic field is also shown in Figure 2b. The geographic correlation between the origins of the protons and the magnetic field of LMA seen in Figure 2 indicates that the source location of the observed protons are associated with the LMAs in the Southern Hemisphere that are located close to the SPA basin.

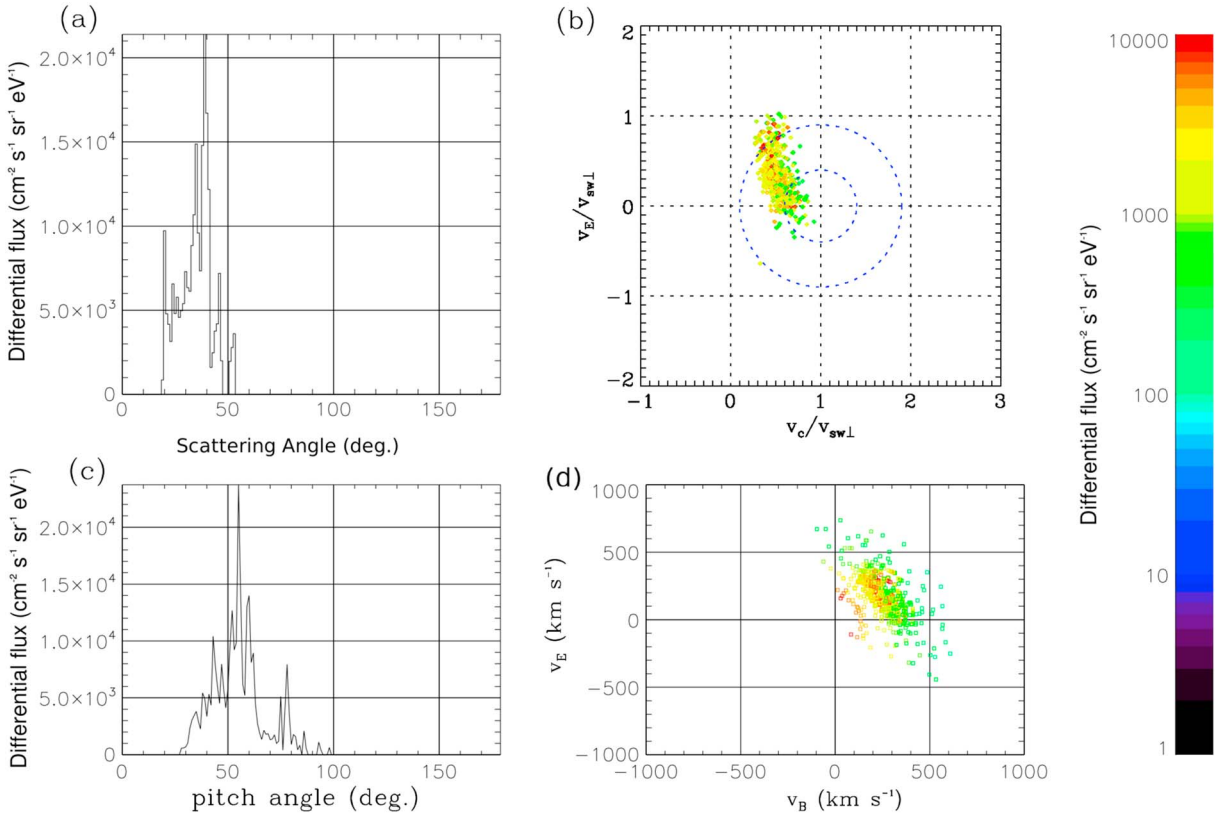

Figure 3. Distributions for population *C* in orbit 1977. (a) Calculated scattering angle distribution. Here the scattering angle is defined as the angle between the incident solar wind velocity vector and the velocity vector of protons that hit the lunar surface at the end of backtracing (i.e., protons scattered from lunar magnetic anomaly). (b) Velocity distribution normalized with the component of the solar wind velocity perpendicular to the IMF ($v_{sw_\perp}$). The component of velocity of protons parallel to the drift velocity ($\vec{E_c} \times \vec{B_{IMF}}$) is shown on the horizontal axis (v_c) and that parallel to E_c (v_E) is shown on the vertical axis. The value of $v_{sw_\perp}$ is averaged during the observation of population *C* and is ~400 km/s. (c) Measured pitch angle distribution. (d) Velocity distribution in v_E-v_B plane, where v_B is the velocity component parallel to B_{IMF} for the protons of population *C*.

Such observations are recorded during several but not all orbits between 19 and 21 April 2009 when Chandrayaan-1 orbit was very similar (details presented in Table 1 in the supporting information). This suggests that the observations of these protons at low altitude on the lunar nightside are highly dependent upon the background solar wind conditions such as IMF and solar wind velocity. The important criterion for the observation of the protons during terminator crossing is found to be the presence of the small negative *z* component of IMF (B_z) in the aLSE frame. The protons were observed only in those orbits for which B_z was negative during the terminator crossing. Another important criterion of the observation is found to be the presence of either a dominant positive (B_y) component or a dominant negative (B_x) component. We found that observations of proton populations similar to *C* takes place for $-50° \leq \theta_B \leq 0°$ and $\phi_B \geq 70°$ (mostly with $\phi_B > 120°$, as described in Table 1 in the supporting information). During the observation of a similar population in the orbit 1980 of Chandrayaan-1 (discussed in the supporting information), the orientation of IMF was such that (θ_B, ϕ_B) ~(−10°, 167°). Few more events are discussed in the supporting information.

4. Discussion

Scattering of solar wind protons from the regions of strong lunar magnetic anomalies on the dayside of the Moon has been reported by the recent lunar missions, such as Chandrayaan-1 (Lue et al., 2011), Kaguya (Saito et al., 2012), and Acceleration, Reconnection, Turbulence, and Electrodynamics of the Moon's Interaction with the Sun (ARTEMIS; Poppe et al., 2017) as well as suggested by Nozomi observations in the past at large distance from the Moon (Futaana et al., 2003). The maximum reflection efficiency were found to be as high as 50% with a global average of ~10% (Lue et al., 2011), while the unmagnetized lunar surface can reflect only

0.1 – 1% of the solar wind flux (Holmström et al., 2010; Saito et al., 2008). The backtracing shows a clear association of the protons of population *C* observed by SWIM in orbit 1977 from their point of observation in the near wake region back across the terminator to the location of the lunar magnetic anomaly near the SPA, suggesting that these protons are most likely solar wind protons scattered by the magnetic anomaly. Such protons, after scattering, travel under the influence of the electromagnetic forces of IMF and CEF and the resulting trajectories allow them to access the near wake region where they have been detected by the SWIM.

Recently, from ARTEMIS observations, Poppe et al. (2017) have shown that the angular scattering function for the scattering of solar wind protons by LMAs depends on the SZA in such a way that the scattering is isotropic at low SZAs and becomes more of a forward scattering at high SZAs. During the events observed by SWIM reported in this paper, the protons mostly originated from the SPA LMA spread across 140° – 200° longitude and correspond to SZA of 90° – 40° for subsolar point located at 240° longitude. Thus, it is plausible to assume that the SPA LMA would have scattered solar wind protons in the forward direction and these protons, by virtue of their trajectories under IMF and CEF, reached the near wake region where SWIM has detected these ions as population *C*. Since the backtracing model computes the velocity of the observed protons at each time step along the trajectory, the angle between the velocity of these protons and that of the incoming solar wind protons are computed when the protons hit the lunar surface at the end of backtracing. This angle can be considered as an estimate of the scattering angle at LMAs, and the distribution of which is shown in Figure 3a. Figure 3a shows the scattering angles to be <90°, with a peak around 50°, supporting forward scattering, which agrees with Poppe et al. (2017).

The observation of this population is highly contingent upon the background solar wind and IMF conditions. The dominant positive B_y during observation ensures that the forward scattered protons at SPA will gyrate toward South Pole and thereby access the near wake crossing the south pole of the Moon. The dominant positive E_z component of the CEF during the observation of such protons means that the protons traveling across the South Pole would experience a decelerating force, actually deflecting the trajectories toward the lunar surface. This in turn can explain the lower energy of population *C* compared to that of solar wind.

We estimated the flux of the protons of population *C* observed in orbit 1977, assuming an angular pixel size of 30° (Lue et al., 2011) and found it to be 1.0×10^5 cm^{-2}·s^{-1}. The solar wind proton flux during the observation was 2.0×10^8 cm^{-2}·s^{-1}. Thus, the observed flux is 5×10^{-4} of the solar wind proton flux. This is a small fraction of the global average of the reflection ratio for solar wind protons scattered from the LMAs (Lue et al., 2011). This could be due to the fact that protons are found to originate from a broader region on the lunar surface where the SZA varies from 90° to 50°. At lower SZA, isotropic scattering will be significant compared to the forward scattering (Poppe et al., 2017), which means protons will be scattered nearly over 2π and not all of them would reach the nightside. Further, the protons that are scattered at the SPA LMA and transported across the terminator will have a range of trajectories of which only a small fraction is detected by SWIM.

Ions produced in a stationary frame such as the Moon with respect to the moving solar wind frame start to gyrate around the IMF and drift toward the $\vec{E_c} \times \vec{B_{\mathrm{IMF}}}$ direction, where the CEF $\vec{E_c} = -\vec{V_{\mathrm{sw}}} \times \vec{B_{\mathrm{IMF}}}$ is produced due to the relative motion of the two frames. The total motion of the ions is given by the superposition of the gyration and the drift motion. For a large population of gyrating and drifting ions, a ring-shaped velocity distribution centered at $(v_{\mathrm{sw}_\perp}, 0)$ is expected in the v_c-v_E plane, where v_c is the velocity component of the ions parallel to the $\vec{E_c} \times \vec{B_{\mathrm{IMF}}}$ drift, v_E is the velocity component of the ions parallel to E_c, and $v_{\mathrm{sw}_\perp}$ is the component of the solar wind velocity perpendicular to B_{IMF}. For ions with zero initial velocity, the radius of the distribution is expected to be $v_{\mathrm{sw}_\perp}$. For protons with finite initial velocity, the radius of the distribution would be greater than $v_{\mathrm{sw}_\perp}$ if the initial velocity is antiparallel to the solar wind velocity and smaller than $v_{\mathrm{sw}_\perp}$ if the initial velocity is parallel to the solar wind velocity. Figure 3b shows the velocity distribution of the observed protons in the v_c-v_E plane normalized with $v_{\mathrm{sw}_\perp}$. The distribution is partially ring shaped with center at (+1, 0) and radius in the range $(0.4 – 0.8) \times v_{\mathrm{sw}_\perp}$, suggesting that the observed protons have traveled under the influence of E_c and B_{IMF} and have finite initial velocities with significant component parallel to the solar wind velocity vector ($-x$ axis of aLSE coordinates). This is in agreement with the interpretation that the observed protons in near wake are the solar wind protons that are forward scattered from LMAs (in aLSE coordinates). The component of velocity of the observed protons parallel and perpendicular to B_{IMF} is almost equivalent, and this is manifested in the pitch angle distribution shown in Figure 3c, which peaks at ~50°. The velocity distribution in the v_B-v_E plane, where v_B being the component of the proton velocity parallel to B_{IMF}, presented in Figure 3d shows significant

spread in v_B, indicating the range of velocities the protons would have had after scattering. Further, SWIM had observed these protons inside the wake and during terminator crossings, where other electromagnetic fields such as wake boundary electric field are also present, which can change the proton distribution significantly.

Transport of the solar wind protons scattered from the dayside lunar surface into the near wake region deeper inside (close to the antisubsolar point), known as type-II entry mechanism, has been reported from Kaguya observations (Nishino et al., 2009). These protons are picked up by the solar wind and hence gain access to deeper locations inside the wake. The protons observed by the SWIM are less likely to be associated with type II since these originate from LMA instead of lunar surface. Also, the source location of the observed protons are found near to the terminator region very close to the wake boundary.

Thus, the observation reported here demonstrates for the first time the transport of solar wind protons into the near wake region after scattering from the SPA magnetic anomaly. The flux of these protons is comparable to the fraction of the solar wind protons that enter into the near wake region by other known processes (similar to population *B*) such as reported by Dhanya et al. (2013, 2016) and hence is a significant source. ARTEMIS observations have shown the proton reflection ratio from SPA LMA to be 12% (Poppe et al., 2017). We show that out of these reflected protons from the SPA, a certain fraction of them indeed reaches the nightside, and also, we quantified the flux and energy of such a population. Recent studies have shown that due to the interaction of protons in near wake region with the nightside lunar surface, energetic neutral atoms are produced (Vorburger et al., 2016), and that the nightside surface charging can be affected due to the emission of secondary electrons (Nishino et al., 2017). The plasma in the near wake region generate instabilities and significantly affect the electromagnetic environment of Moon (Nishino et al., 2010). The knowledge of the near lunar wake plasma environment is still evolving and the understanding of different plasma populations, with their range of energies and flux involved, are very essential for any future efforts to characterize and advance our knowledge about the lunar plasma environment. Thus, the observations reported in this paper provide a vital input in this direction.

The plasma distribution in the near wake region due to the protons scattered from LMA will be highly asymmetrical because the SZA of the prominent LMAs are continuously changing during the lunar orbit. This calls for detailed studies in the future under varying SZA and IMF conditions.

To test the sensitivity of B_{IMF}, E_c, and wake boundary electric field on the computed trajectories of the protons using our backtracing model, we have done the sensitivity analysis. The analysis was done by varying the magnitude of B_{IMF} and the wake boundary electric field. Further, the impact of the time shift involved in using the solar wind parameters observed at L1 point of Sun-Earth system was also analyzed. The analysis showed that the results are not changed significantly, and hence, the interpretations remain the same. These details are presented in the supporting information. Our model does not incorporate magnetic and electric fields associated with LMA. Since, such a field would affect mostly the proton trajectories very close to the lunar surface, we have chosen coarse grid size of $5° \times 5°$ to avoid influence of LMA field in our trajectory computations.

5. Conclusion

A population of ions with wide angular distribution was observed across the terminator and in the near wake region of the Moon by the SWIM/SARA onboard Chandrayaan-1. The analysis of these ions in several orbits shows that these are basically protons with $m/q = 1$. These observations were made when Chandrayaan-1 spacecraft was passing close to the SPA basin at nightside of the Moon while SPA itself was on the dayside. The backtracing of these protons suggest that they originate from the large lunar magnetic anomaly located close to the SPA. During these observations, the SZA was relatively large ($\sim$40° – 90°) at the magnetic anomaly. We interpret that the observed protons are the solar wind protons that are forward scattered from the magnetic anomaly located at SPA. The angle between the velocity of the protons that hit the lunar surface at the end of backtracing and that of the solar wind protons indicate the process to be more of forward scattering. We found that the orientation of the IMF and the CEF play an important role in the observation of these protons by SWIM. The observed flux of these protons is $\sim 5 \times 10^{-4}$ of the solar wind proton flux, which is comparable to the fraction of the solar wind protons that enter into the near wake region by other known processes. Such protons can significantly affect the electromagnetic environment in the near wake region. These are the first observations revealing the transport of solar wind protons scattered from lunar magnetic anomalies into the near wake region of Moon.

Acknowledgments
The authors thank the ACE SWEPAM instrument team, ACE MAG instrument team, and the ACE Science Center for providing the ACE data. We thank the WIND team and MIT Space Plasma Group for the WIND data (ftp://space.mit.edu/pub/plasma/wind/kp_files/). Chandrayaan-1 data are available for public at Indian Space Science Data Center (ISSDC; https://www.issdc.gov.in/chandrayaan1.html). The efforts at Space Physics Laboratory of Vikram Sarabhai Space Centre are supported by Indian Space Research Organization (ISRO) and at the Physical Research Laboratory by the Department of Space. Abhinaw Alok gratefully acknowledges ISRO and Director, SPL for the research support provided during the period in which this work was conducted. The effort at the University of Bern was supported in part by ESA and by the Swiss National Science Foundation.

References

Barabash, S., Bhardwaj, A., Wieser, M., Sridharan, R., Kurian, T., Varier, S., et al. (2009). Investigation of the solar wind-Moon interaction onboard Chandrayaan-1 mission with the SARA experiment. *Current Science*, *96*(4), 526–532.

Bhardwaj, A., Barabash, S., Futaana, Y., Kazama, Y., Asamura, K., McCann, D., et al. (2005). Low energy neutral atom imaging on the Moon with the SARA instrument aboard Chandrayaan-1 mission. *Journal of Earth System Science*, *114*, 749–760. https://doi.org/10.1007/BF02715960

Bhardwaj, A., Dhanya, M. B., Alok, A., Barabash, S., Wieser, M., Futaana, Y., et al. (2015). A new view on the solar wind interaction with the Moon. *Geoscience Letters*, *2*, 10. https://doi.org/10.1186/s40562-015-0027-y

Bhardwaj, A., Dhanya, M. B., Sridharan, R., Barabash, S., Yoshifumi, F., Wieser, M., et al. (2012). Interaction of solar wind with Moon: An overview on the results from the SARA experiment aboard Chandrayaan-1. *Advances in Geosciences*, *30*, 35–55. https://doi.org/10.1142/9789814405744_0004

Colburn, D. S., Currie, R. G., Mihalov, J. D., & Sonett, C. P. (1967). Diamagnetic solar wind cavity discovered behind the Moon. *Science*, *158*, 1040–1042. https://doi.org/10.1126/science.158.3804.1040

Dhanya, M. B., Bhardwaj, A., Futaana, Y., Barabash, S., Alok, A., Wieser, M., et al. (2016). Characteristics of proton velocity distribution functions in the near-lunar wake from Chandrayaan-1/SWIM observations. *Icarus*, *271*, 120–130. https://doi.org/10.1016/j.icarus.2016.01.032

Dhanya, M. B., Bhardwaj, A., Futaana, Y., Barabash, S., Wieser, M., Holmström, M., & Wurz, P. (2017). New suprathermal proton population around the moon: Observation by sara on chandrayaan-1. *Geophysical Research Letters*, *44*, 4540–4548. https://doi.org/10.1002/2017GL072605

Dhanya, M. B., Bhardwaj, A., Futaana, Y., Fatemi, S., Holmström, M., Barabash, S., et al. (2013). Proton entry into the near-lunar plasma wake for magnetic field aligned flow. *Geophysical Research Letters*, *40*, 2913–2917. https://doi.org/10.1002/grl.50617

Futaana, Y., Barabash, S., Wieser, M., Holmström, M., Bhardwaj, A., Dhanya, M. B., et al. (2010). Protons in the near-lunar wake observed by the Sub-keV Atom Reflection Analyzer on board Chandrayaan-1. *Journal of Geophysical Research*, *115*, 248. https://doi.org/10.1029/2010JA015264

Futaana, Y., Machida, S., Saito, Y., Matsuoka, A., & Hayakawa, H. (2003). Moon-related nonthermal ions observed by Nozomi: Species, sources, and generation mechanisms. *Journal of Geophysical Research*, *108*(A1), 1025. https://doi.org/10.1029/2002JA009366

Halekas, J. S., Bale, S. D., Mitchell, D. L., & Lin, R. P. (2005). Electrons and magnetic fields in the lunar plasma wake. *Journal of Geophysical Research*, *110*, A07222. https://doi.org/10.1029/2004JA010991

Holmström, M., Wieser, M., Barabash, S., Futaana, Y., & Bhardwaj, A. (2010). Dynamics of solar wind protons reflected by the Moon. *Journal of Geophysical Research*, *115*, 206. https://doi.org/10.1029/2009JA014843

Lue, C., Futaana, Y., Barabash, S., Wieser, M., Holmström, M., Bhardwaj, A., et al. (2011). Strong influence of lunar crustal fields on the solar wind flow. *Geophysical Research Letters*, *38*, 202. https://doi.org/10.1029/2010GL046215

Mitchell, D. L., Halekas, J. S., Lin, R. P., Frey, S., Hood, L. L., Acuña, M. H., & Binder, A. (2008). Global mapping of lunar crustal magnetic fields by Lunar Prospector. *Icarus*, *194*, 401–409. https://doi.org/10.1016/j.icarus.2007.10.027

Nishino, M. N., Fujimoto, M., Maezawa, K., Saito, Y., Yokota, S., Asamura, K., et al. (2009). Solar-wind proton access deep into the near-Moon wake. *Geophysical Research Letters*, *36*, 103. https://doi.org/10.1029/2009GL039444

Nishino, M. N., Fujimoto, M., Saito, Y., Yokota, S., Kasahara, Y., Omura, Y., et al. (2010). Effect of the solar wind proton entry into the deepest lunar wake. *Geophysical Research Letters*, *37*(L12), 106. https://doi.org/10.1029/2010GL043948

Nishino, M. N., Harada, Y., Saito, Y., Tsunakawa, H., Takahashi, F., Yokota, S., et al. (2017). Kaguya observations of the lunar wake in the terrestrial foreshock: Surface potential change by bow-shock reflected ions. *Icarus*, *293*, 45–51. https://doi.org/10.1016/j.icarus.2017.04.005

Nishino, M. N., Maezawa, K., Fujimoto, M., Saito, Y., Yokota, S., Asamura, K., et al. (2009). Pairwise energy gain-loss feature of solar wind protons in the near-Moon wake. *Geophysical Research Letters*, *36*, 108. https://doi.org/10.1029/2009GL039049

Poppe, A. R., Halekas, J. S., Lue, C., & Fatemi, S. (2017). ARTEMIS observations of the solar wind proton scattering function from lunar crustal magnetic anomalies. *Journal of Geophysical Research: Planets*, *122*, 771–783. https://doi.org/10.1002/2017JE005313

Purucker, M. E., & Nicholas, J. B. (2010). Global spherical harmonic models of the internal magnetic field of the Moon based on sequential and coestimation approaches. *Journal of Geophysical Research*, *115*, E12007. https://doi.org/10.1029/2010JE003650

Saito, Y., Nishino, M. N., Fujimoto, M., Yamamoto, T., Yokota, S., Tsunakawa, H., et al. (2012). Simultaneous observation of the electron acceleration and ion deceleration over lunar magnetic anomalies. *Earth Planets Space*, *64*, 83–92. https://doi.org/10.5047/eps.2011.07.011

Saito, Y., Yokota, S., Asamura, K., Tanaka, T., Nishino, Y. M. N., Terakawa, Y., et al. (2010). In-flight Performance and Initial Results of Plasma Energy Angle and Composition Experiment (PACE) on SELENE (Kaguya). *Space Science Reviews*, *154*, 265–303. https://doi.org/10.1007/s11214-010-9647-x

Saito, Y., Yokota, S., Tanaka, T., Asamura, K., Nishino, M. N., Fujimoto, M., et al. (2008). Solar wind proton reflection at the lunar surface: Low energy ion measurements by MAP-PACE onboard SELENE (KAGUYA). *Geophysical Research Letters*, *35*, 205. https://doi.org/10.1029/2008GL036077

Vorburger, A., Wurz, P., Barabash, S., Futaana, Y., Wieser, M., Bhardwaj, A., et al. (2016). Transport of solar wind plasma onto the lunar nightside surface. *Geophysical Research Letters*, *43*, 10,586–10,594. https://doi.org/10.1002/2016GL071094

Wang, X.-D., Bian, W., Liu, J. J., Zou, Y. L., Zhang, H. B., Lü, C., et al. (2010). Acceleration of scattered solar wind protons at the polar terminator of the Moon: Results from Chang'E-1/SWIDs. *Geophysical Research Letters*, *37*, 203. https://doi.org/10.1029/2010GL042891